Fig. 1 Invariant Points in Cr-Fe-Ni Ternary System from [4], [5] and [7]

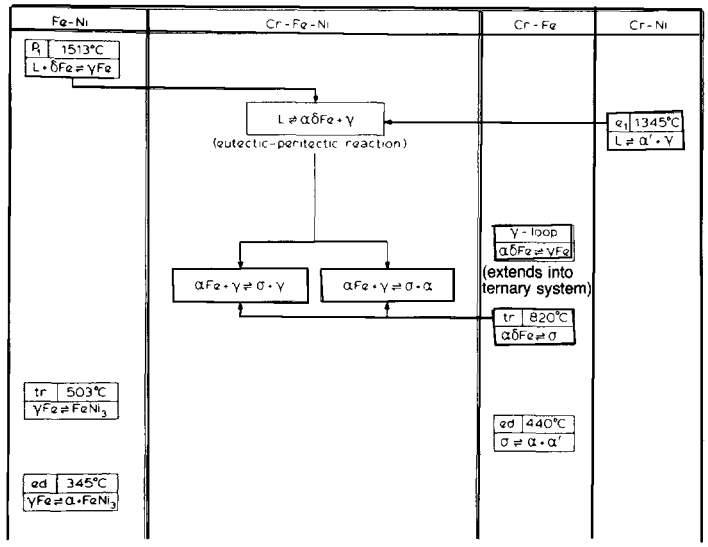

e, eutectic; ed, eutectoid; p, peritectic; tr, transformation. From [Rivlin/Raynor], 1980.

Table 1 Allotropes of Iron

Temperature range, °C	Symbol	Crystal structure	Pearson lattice designation
1536–1392	δFe	bcc	*cI*2
1392–911	γFe	fcc	*cF*4
911 and below	αFe	bcc	*cI*2

Cr. The element is bcc below its melting point. The melting point itself is somewhat uncertain: its high value, approaching 1900 °C, and the reactivity of the element have made the exact magnitude difficult to determine. A careful review of the original literature of [2] places the melting point at a mean of 1878 ± 22 °C. Solid solutions in chromium are denoted α'. When the bcc solid solutions in iron and chromium are continuous, as is the case over 1000 °C, the symbol α is used. Claims for allotropy in chromium have been published from time to time and are reviewed by [Pearson]. However, the balance of the evidence leaves little doubt that the structure is bcc at all temperatures below the melting point.

Ni. The element is fcc below its melting point (1453 °C) and has a ferromagnetic Curie temperature of between 352 and 360 °C [1]. Solid solutions in nickel are given the symbol γ and are continuous with solid solutions in fcc iron.

Binary Systems

The diagrams for the Cr-Fe, Cr-Ni and Fe-Ni systems, which are presented separately in this issue of the Bulletin, rely on [Hansen], [Elliott] and [Shunk], with information from more recent investigations also being considered in their construction.

Ternary System

The long-standing importance of Cr-Fe-Ni in ferrous metallurgy has resulted in the constitution of this alloy system being one of the most thoroughly investigated among iron ternary systems.

Early work is summarized in a very comprehensive metallographic survey by [3]. The range defined by the Fe corner, 30 wt.% Ni, and 60 wt.% Cr was identified and mapped out for C contents of 0.05-0.5%. Four solid phases were identified as follows:

- **Solid solutions**
  - γ fcc based on γ Fe and Ni
  - α bcc based on α Fe
  - α' bcc based on Cr
- **Intermetallic phase**
  B: a hard, brittle, and non-magnetic phase (subsequently identified as σ), and derived from the Cr-Fe edge. The 'B phase' did not form at Ni contents above about 10% nor above 900 °C but did occur over a very wide range of Cr contents. Reac-

Fig. 2 Liquidus Projection of Cr-Fe-Ni System from [4], [5] and [7]

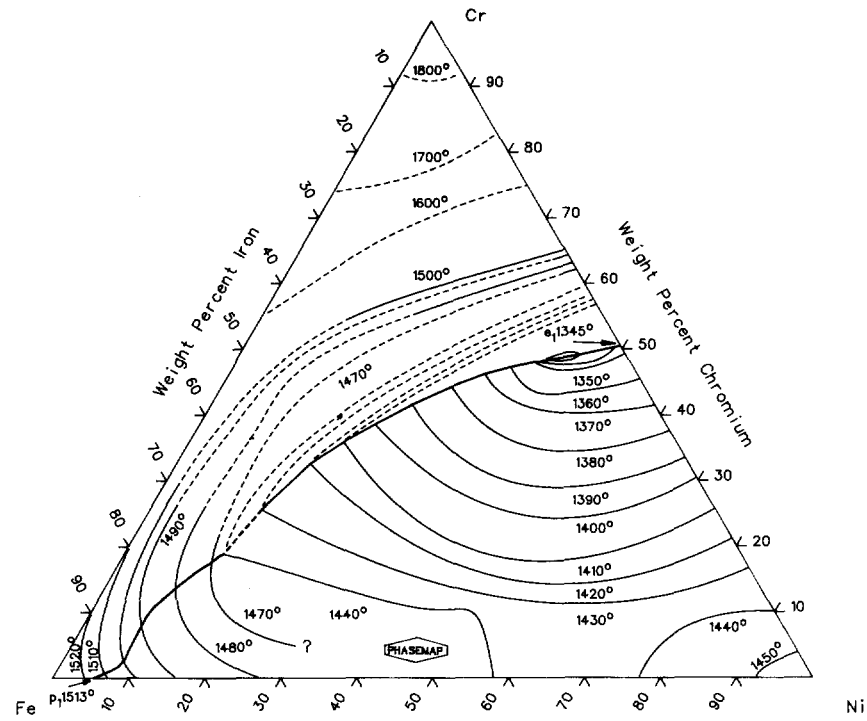

From [Rivlin/Raynor], 1980.

tions forming B were sluggish. The general picture given by [3] is essentially correct, apart from the absence of a low-temperature limit to the stability of the B-phase. Later work is devoted to pinpointing phase-boundary positions.

Surveys of the liquidus and solidus by [4–7] show that a transition from peritectic to eutectic equilibrium occurs as compositions change from the Fe-Ni to the Cr-Ni edge. A univariant reaction line may be drawn from the Fe-Ni peritectic ($L + \delta \leftrightharpoons \gamma$) to the Cr-Ni eutectic ($L \leftrightharpoons \alpha' + \gamma$). On the Fe-Ni side of the line a gradual slope to the Fe-Ni edge is found. On the opposite side, the liquidus rises steeply to the Cr-Fe and Cr-Ni edges. Solidification reactions form γ and α.

Semi-quantitative measurements of the extent of the σ-phase by [8, 9] confirm that the intermetallic compound σ plays no part in the melting equilibria and that it does not form at Ni contents above about 12%. A congruent transformation of σ to α between 900 and 1000 °C is reported, i.e., the ternary σ-phase is stable at higher temperatures than in the binary Cr-Fe system.

Invariant points are summarized in Fig. 1.

Quantitative measurements of the isotherms from 1300 to 650 °C and approximately at 550 °C by [10-20] are in general agreement on the identity of all phases (see also "Crystal Structures" in the Cr-Fe, Cr-Ni and Fe-Ni Systems). Discrepancies in the location of the phase boundaries mainly revolve around the sluggishness of reactions forming σ and the effects of cold work and alloy purity. At low temperatures the α-, α'- and σ-phases are found toward the Cr-Fe edge while the γ-phase dominates the Ni-corner. The upper temperature limit of σ is at about 950 °C [17, 18] while the solid phases in equilibrium between 950 °C and the melting point are γ and α (where α is a continuous solid solution between α Fe, δ Fe, and α').

[21] have obtained experimental results for the mechanical properties over a wide composition range and reviewed them in the light of previous work on the phase equilibria. In addition, they analyzed the system by means of a series of polytherms taken at constant iron contents from 10 to 90 wt.% Fe (see also [5] for a similar approach). An extensive survey and bibliography of the physical metallurgy of corrosion-resistant alloys comprising the Cr-Fe-Ni system may also be found in [22].

Liquidus and Solidus

The major contributions are contained in [4], [5] and [7]. The main regions were surveyed by [5] using thermal and dilatometric analyses from the Cr-Ni edge up to 95 wt.% Fe. A liquidus surface with an univariant line running from the Fe-Ni peritectic to the Cr-Ni eutectic was established, with a gradual slope on one side up to the melting point of Ni. The purity of the alloys was not very high; the silicon content was sometimes in excess of 1% though in most cases of the order 0.1%. [7] surveyed the same area and gave a very similar surface using materials carefully selected for purity: i.e., electrolytic Fe, selected shot Ni, and either thermit or electrolytic Cr. Alloys were made by melting under H_2 and analyses showed insoluble matter, $Cr_2O_3 < 0.75\%$ and $Si < 0.16\%$. Thermal analyses were accurate to ± 5 K

Fig. 3 Solidus Projection of Cr-Fe-Ni System from [4], [5] and [7]

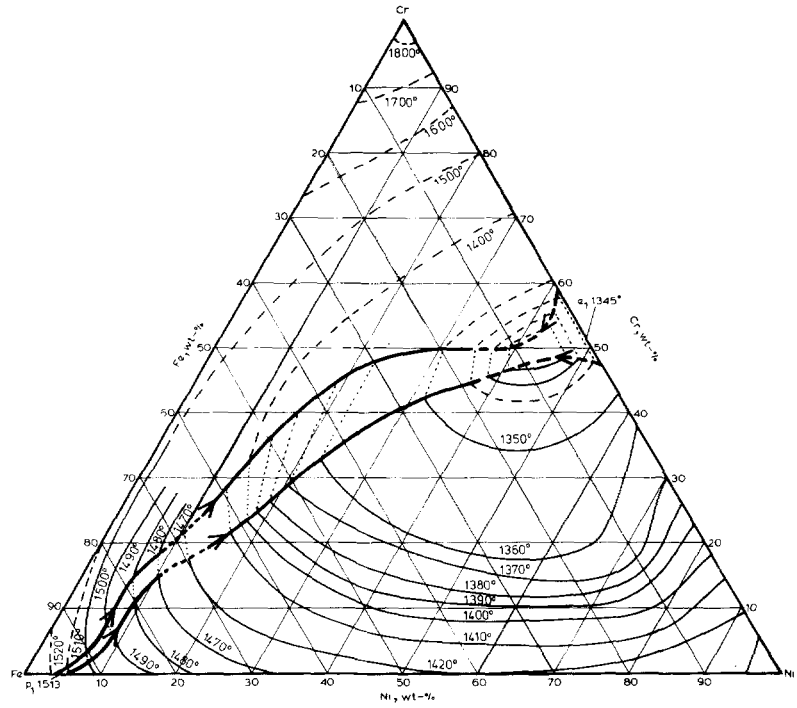

From [Rivlin/Raynor], 1980.

and the solidus measurements were supplemented by metallographic examination of annealed and quenched samples. The results from [5] and [7] are broadly in agreement but in some cases with discrepancies of the order 20 K.

The investigations of [4] are confined to the Fe corner in a region bounded by 21 wt.% Ni and 33 wt.% Cr and combine microprobe-analysis measurements of quenched specimens with supplementary thermal analyses. Purities are not specified precisely: 'technically pure' iron, electrolytic nickel, and electrolytic chromium. The results agree fairly well with previous work but show an 'S' bend on the projection of the univariant line.

Figures 2 and 3 combine data from [4], [5] and [7]. The detailed presentation of [4] encourages a favorable comparison with that of [7], the contours of which have been adjusted accordingly. In many instances, no experimental points exist to define the precise location of contours, which are indicated, therefore, by dashed lines. As far as possible, the ternary surface was made consistent with the accepted binary constitution at the edges of the diagrams but anomalies remain: see for example, the Fe-Ni edge, which disagrees with the 1470 °C contour. Liquidus and solidus temperatures are quoted for three alloys by [23], which exceed those predicted by Fig. 2 and 3 by 10 to 55 K according to composition.

The liquidus in [6] and [7] has a minimum in the univariant reaction line located at a temperature just below 1300 °C and at 49 wt.% Cr-8 wt.% Fe-43 wt.% Ni. The minimum, corroborated by solidus experiments, is described as a 'depressed binary eutectic point' and was represented by [7] as a reaction in which solid solution is of the same composition as the liquid with which it is in equilibrium. The possibility that it is an invariant eutectic reaction requires four phases, one liquid and three solid, but only two solid phases occur along the univariant valley line, γ and α (the separate phases α and α' exist only at lower temperatures). An alternative interpretation discussed in [7] postulates the development of a critical tie-line at the minimum (see [24]), and this interpretation is adopted in the representation of the solidus in Fig. 3.

Isothermal Solid Sections

The phase boundaries defining equilibria between the four solid phases α, α', γ and σ have been the subject of quantitative investigations from 1300 to 650 °C. A selection is given in Fig. 4 to 6. Estimated boundaries for 550 °C have been reproduced in Fig. 7.

There is qualitative agreement among most publications as to the number and structure of phases present and their approximate composition limits at different temperatures. The influence of the σ-phase upon equilibria in the solid is the crucial factor. The stability limits of σ are not well defined even in the binary Cr-Fe system, where the low-temperature eutectoidal transformation was established for the first time in 1957. The discrepancies between different papers for the composition limits of the σ-phase in the ternary system are due largely to different experimental conditions [10–14,

Fig. 4 High-Temperature Isotherms of Cr-Fe-Ni System

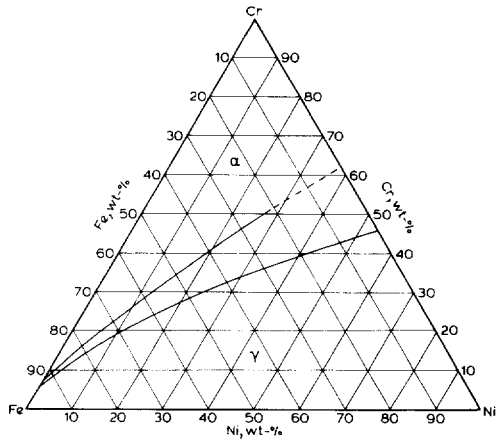

At 1300 °C; from [16].

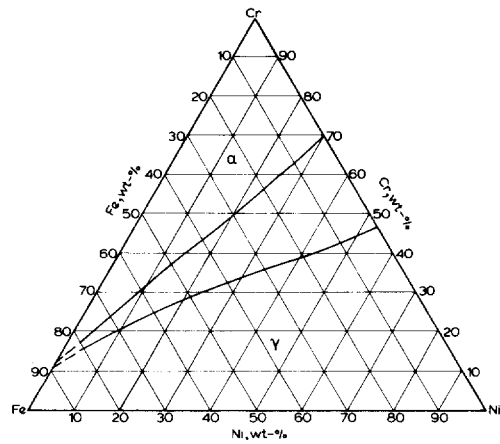

At 1200 °C; from [19] and [20].

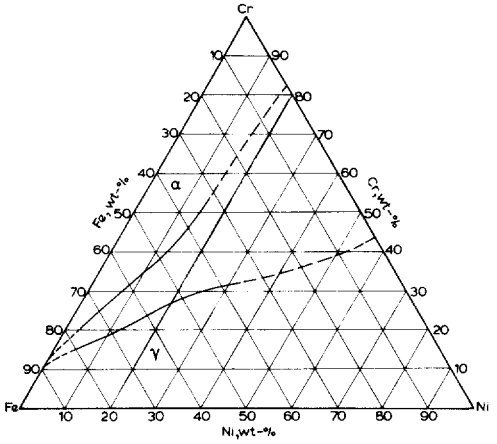

At 1100 °C; from [20].

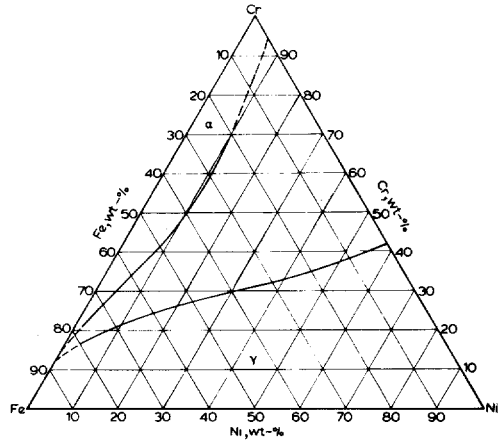

At 1000 °C; from [20].

From [Rivlin/Raynor], 1980.

17, 18]. No single publication can claim a definitive phase diagram for the Cr-Fe-Ni system in the solid state. In the following sections, adaptations have been made from the more reliable papers in drawing a set of self-consistent isotherms.

Isotherms from 1300 to 1000 °C (Fig. 4)

Solid-phase equilibria between 1300 and 1000 °C are determined solely by the co-existence of γ (fcc) and α (bcc). At 1300 °C a careful microscopical measurement by [16] was made of the $\alpha / (\alpha + \gamma)$ and $(\alpha + \gamma) / \gamma$ boundaries using alloys of moderately high purity, annealed in vacuo for periods of 3–114 h (generally over 50 h) and water quenched. Figure 4 shows that the extrapolation of the $(\alpha + \gamma) / \gamma$ boundary agrees fairly well with the Cr-Ni edge.

Data for the boundaries at 1200 to 1000 °C are reported in [5] and [17–20]. The early work of [5] is vitiated by the relatively low purity of the alloys and the isotherms at 1200, 1100 and 1000 °C (Fig. 4) rely mainly on [19] and [20].

[20] prepared ternary diffusion couples from high-purity metals by annealing in vacuo under argon to equilibrium at 1200, 1100 and 1000 °C. The interface compositions were measured by a standardized microprobe-analysis technique. Deviations from true equilibrium compositions of the interphase boundaries are claimed to be less than 1% because of prolonged heat treatment. The duration, however, was not specified and no mention was made of phase identification. Nevertheless there is excellent agreement, where tem-

Fig. 5 Isotherm of Cr-Fe-Ni System at 900 °C from [8], [14], [17] and [19]

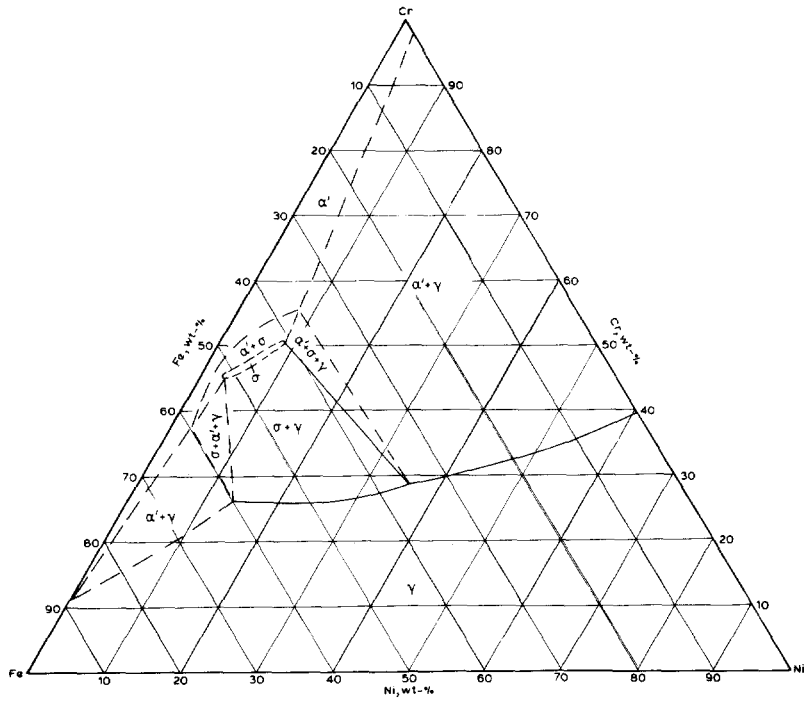

From [Rivlin/Raynor], 1980.

Table 2 Solvus Tie-line Intercepts for $\alpha / (\gamma + \alpha)$ and $\gamma / (\gamma + \alpha)$ Boundaries: Microprobe Analyses of Equilibrated Specimens [19]

	Composition, wt.%			
	$\alpha / (\alpha + \gamma)$		$\gamma / (\gamma + \alpha)$	
Temperature, °C	Fe	Cr	Fe	Cr
1204	0.0	70.0	0.0	47.0
	8.5	64.0	10.0	42.5
	(22.8	57.0	20.0	39.0)(a)
	26.2	51.6	29.8	36.0
	35.6	46.5	38.2	33.0
1260	0.0	64.0	0.0	48.0
	7.6	58.8	8.1	44.0
	16.6	53.8	18.0	40.0
	(27.0	48.5	28.0	35.0)(a)
	38.0	42.4	38.0	33.0

(a) The figures for these intercepts are inconsistent with the smooth graphical presentation given in [19] and may include a misprint.

peratures coincide, with the isotherms in [19]. The latter determined solid solubility in γ at 1260, 1204, 1093, 982, 899 and 816 °C by metallographic examination of high-purity alloys that had been cold worked and annealed to equilibrium (up to 1000 h at the lower temperatures). Data at 1204 °C have been combined with data at 1200 °C from [20] in Fig. 4. Isotherms at 1100 and 1000 °C (Fig. 4) rely entirely on [20]. It is unfortunate that the differences in annealing temperatures used in [19] and [20] prevent direct comparison of compositions in every case. However, compositional variations with temperature are entirely consistent with the trend observed in Fig. 4 where the two-phase (α + γ) field widens as the temperature falls.

[19] made use of microprobe analysis to determine tie-lines at 1260 and 1204 °C, where the grains of individual phases had grown to a size sufficiently large for this technique. The data are given in Table 2. Tie-lines by [20] are given in Table 3. Note that the latter also determined tie-lines at 920 °C but they consider their figures to represent the (α + γ) phase range, whereas it is believed that the σ-phase is stable to at least 950 °C at the relevant compositions (see below). These figures are not included in Table 4.

Isotherms from 900 to 650 °C (Fig. 5 and 6)

The σ-phase in the ternary Cr-Fe-Ni system has an upper temperature limit that is higher than in the binary Cr-Fe system. According to [18], it may be located at 950 to 960 °C on a section of constant composition at 50 wt.% Fe. The 440 °C eutectoidal transformation, which represents the low-temperature limit of the binary Cr-Fe σ-phase presumably extends into the ternary system but the boundaries are unknown.

The 900 °C isotherm (Fig. 5) has been adapted from the data in [8], [14], [17] and [19]. The dashed lines represent modified boundaries from [14], which are correct in principle but have been adjusted to agree with well established data for the ternary system and for the binary edges.

The isotherm at 800 °C (Fig. 6) was first outlined by [8]. X-ray and microscopical work by [10], [17] and [18] with alloys which had been subjected to prolonged anneals

Fig. 6 Low-Temperature Isotherms of Cr-Fe-Ni System

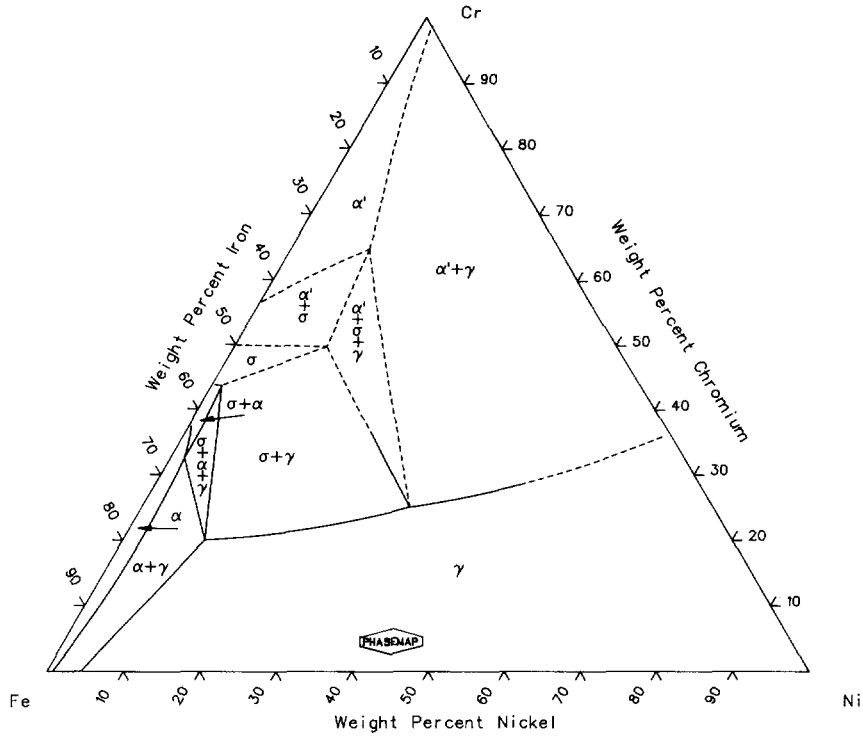

At 800 °C; from [8], [10] and [17].

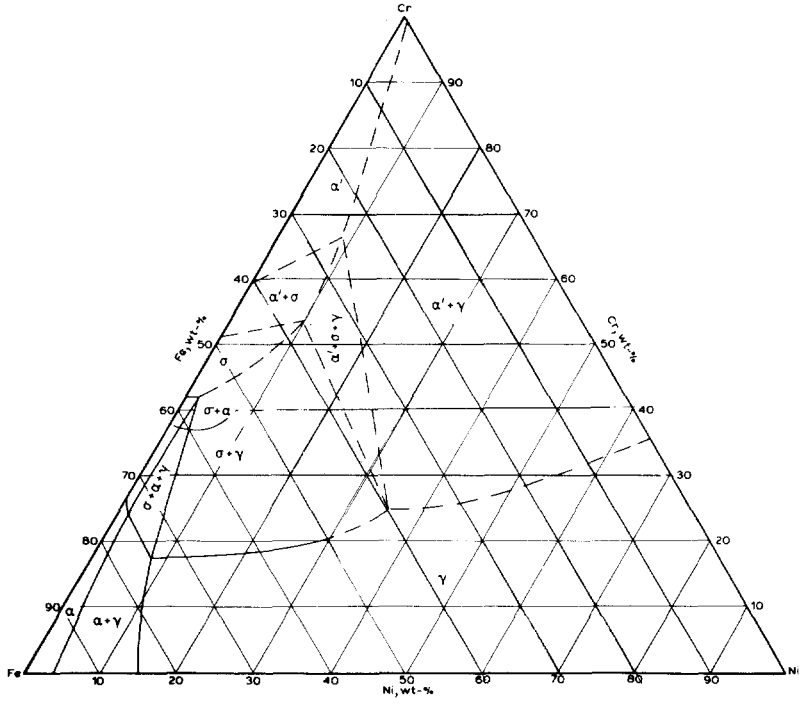

At 650 °C; from [8], [10–12] and [17].
From [Rivlin/Raynor], 1980.

Table 3 Solvus Tie-line Intercepts for $\alpha / (\gamma + \alpha)$ and $\gamma / (\gamma + \alpha)$ Boundaries: Microprobe Analyses of Diffusion Couples [20]

Temperature, °C	Composition, wt.% $\alpha / (\alpha + \gamma)$ Cr	Ni	$\gamma / (\gamma + \alpha)$ Cr	Ni
1200	18.8	3.8	16.6	4.8
	22.0	4.6	18.6	7.3
	26.7	7.5	21.8	11.2
	35.0	11.8	26.8	19.0
	37.1	13.1	27.8	21.2
1100	40.0	12.5	28.2	21.3
	34.7	9.1	24.0	17.0
	29.8	6.9	...	...
	25.0	5.9	17.8	9.5
	19.5	2.7	14.8	3.9
	53.9(a)	14.4(a)	31.8(a)	32.7(a)
1000	33.0	5.5	21.6	12.7
	34.7	7.1	...	...
	44.5	8.7	26.8	21.2
	50.2	10.6	27.2	29.1
	48.2	11.4	28.5	27.3
	50.5	10.9	29.4	26.5
	47.7	10.6	28.0	27.5
	21.0	1.8	16.5	3.5
	25.8	3.4	19.8	5.3
	30.4	4.8	20.7	10.6
	36.7	6.7	24.0	14.9
	41.4	8.9	25.5	19.6
	64.9	10.6	32.4	38.6
	65.6	10.1	32.3	40.1
	59.1(a)	10.8(a)	30.6(a)	32.3(a)

(a) Results for two-phase alloys.

Table 4 Experimental Information on α / γ Equilibrium in Cr-Fe-Ni System [33]

Temperature, °C	Composition, wt.% $\alpha / (\alpha + \gamma)$ boundary Cr	Ni	$\gamma / (\gamma + \alpha)$ boundary Cr	Ni	Reference
850	24.89	2.33	18.26	5.16	34
	22.51	1.72	17.60	4.13	34
	22.70	1.63	17.98	4.21	34
	16.55	4.88	14.10	1.19	34
	17.79	4.99	15.15	1.18	34
1000	36.4	7.7	23.6	16.1	35
	28.3	6.3	19.9	8.6	35
	33.7	8.9	24.8	15.7	35
1200	26.7	6.3	19.3	8.9	35
	30.7	9.8	24.4	14.8	35
1300	24.0	8.1	19.4	11.0	35
	35.5	15.4	28.8	21.5	35
1345	16.1	3.2	14.9	4.1	36
1350	19.6	6.8	17.1	9.0	36
	26.3	9.9	21.8	13.7	36
	21.3	9.1	18.6	12.1	36
1400	9.1	2.1	8.4	3.4	36

and intermediate cold work provided a set of boundaries for Fe-rich alloys. The $\gamma + \alpha + \sigma$ triangle and the two-phase field $(\alpha + \gamma)$ in Fig. 6 are due to [10]. The location of the $\gamma / (\gamma + \sigma)$ boundary is in excellent agreement with [17]. The partial $\gamma / (\alpha' + \gamma)$ boundary of [10] may be extrapolated to meet the Cr-Ni edge at a composition of 36 wt.% Cr, quite consistent with the value of 39 wt.% Cr for the accepted binary system. The remaining

Fig. 7 Estimated Boundaries of Cr-Fe-Ni System at 550 °C from [11]

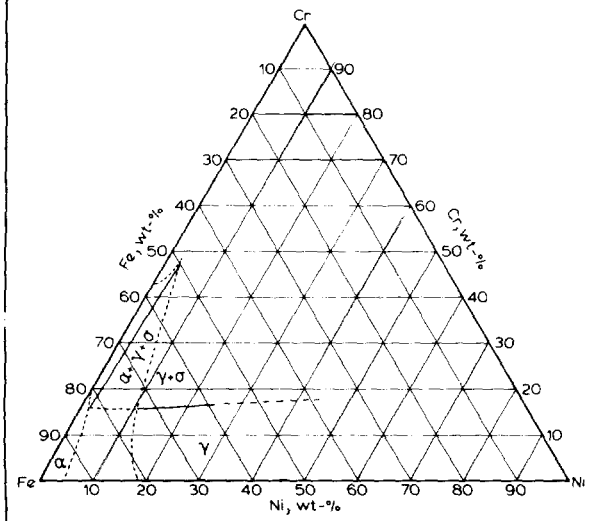

Measured apex from intersection of $(\gamma + \sigma) / (\alpha + \gamma + \sigma)$ with $\gamma / (\gamma + \sigma)$ is 11.5 wt.% Ni and 15.5 wt.% Cr. From [Rivlin/Raynor], 1980.

boundaries, shown as dashed lines, have been adjusted from the work of [8] to agree with the binary edges Cr-Fe and Cr-Ni.

At 650 °C the phase equilibria (Fig. 6) have been the subject of many studies [8, 10–13, 17, 18]. The $\gamma + \alpha + \sigma$ triangle is well defined by [10] and [11]. The boundaries of the two-phase regions $(\alpha + \gamma)$ and $(\sigma + \gamma)$ are taken from [11] and are preferred to those of [8] on the grounds of higher alloy purity, length of heat treatment, and use of intermediate cold work. The $\alpha + \gamma$ boundaries are in good agreement with those of [12].

The identity and distribution of the solid phases at low temperatures have been very carefully surveyed by [9] using X-ray diffraction results from a large number of alloys slowly cooled from 900 °C. While the results cannot be described as equilibrium, they are consistent with the above picture and may be used to rationalize equilibrium data.

The precise limits of the σ-phase in the ternary system are still uncertain. A narrow homogeneity range is proposed at 900 °C and below 10 wt.% Ni (Fig. 5). At lower temperatures this range expands to include the Cr-Fe edge (Fig. 6). At lower temperatures still (possibly about 500 °C) one would anticipate a low-temperature limit analogous with that for the Cr-Fe edge. The difficulty of ascertaining true equilibria in this range is attested by the results of [11], whose isotherm at 550 °C (Fig. 7) is only an estimate because strain-free alloys annealed for over 12 months gave diffuse X-ray diffraction patterns.

At higher temperatures, for example 800 °C and above, the advantage of more rapid reaction is offset by the influence of impurities such as silicon which accelerate σ formation and increase the proportion of σ-phase, thus displacing the γ solvus towards lower chromium contents [13, 15]. A not dissimilar effect is caused by

Fig. 8 Isothermal Sections of Cr-Fe-Ni System from [11]

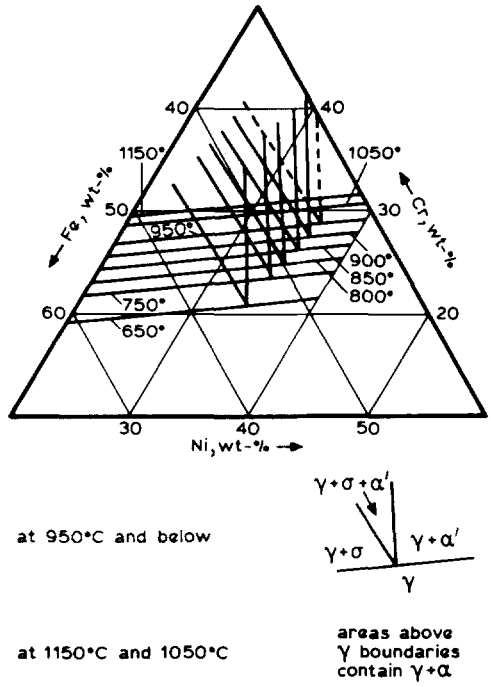

From [Rivlin/Raynor], 1980.

the metals aluminum and titanium [17, 18]. A slight displacement toward higher chromium contents by 0.3 wt.% C has been reported by [14]. The isotherms in Fig. 4–6 are self-consistent when analyzed using polytherms taken at constant iron compositions (10 to 50%). The extent of the γ solvus as studied by [17] and [18] is similarly self-consistent (Fig. 8) and in good agreement with [10] and [11]. However, the boundaries in Fig. 8 should be regarded with some caution. The silicon content was 0.3%, which is high when compared with that in [10] and [11], where the alloys contained silicon in amounts of 0.01% or less. With regard to the location of the γ + σ + α' triangle, [17] used only a limited number of alloys. Furthermore, [19] were unable to repeat an etching technique used by [18] to distinguish α' and σ. For these reasons, the location of the γ apex shown in Fig. 8 is somewhat doubtful.

Thermodynamic Reviews

Direct measurements of basic thermodynamic data for ternary Cr-Fe-Ni alloys may be found in [25]. A study of liquid–vapor equilibria [26, 27] has been presented in the form of ternary activity diagrams from which it is concluded that Cr evaporates from Fe-rich melts at least twice as quickly as from Ni-rich melts. Computer calculations of the ternary system are based largely on data for the binary edges and for the components. A close coincidence of calculated and experimental α / γ boundaries is reported by [28] at 1550 K (1277 °C) and 1373 K (1100 °C). Sections from 1700 K (1427 °C) to 923 K (650 °C) have been calculated by [29, 30], and the results indicate close correspondence between calculated isotherms and direct measurements of ternary alloys. Differences are described as no greater than the discrepancies between different sets of experimental results for binary edges.

Recently, the α / γ boundaries have been recalculated by [20] at 1073 to 1473 K (800 to 1200 °C). A comparison at 1373 K (1100 °C) with their microprobe-analysis results (Table 3) shows close agreement.

Calculations for solid-phase boundaries γ / α, based on experimentally determined activities in the solid state, may be found in [31] for the Fe corner. For the Ni corner, an investigation has been made of activities at 1500 K (1227 °C) using the Knudsen effusion method and microprobe analysis to measure the compositions of samples and condensed layers [32].

[33] investigated the thermodynamics of solution models of the α- and γ-phases in iron alloys. In the instance of the Cr-Fe-Ni system, reasonable agreement is found between the computer-generated isotherm at 1477 K (1204 °C) and the experimental tie-lines of [19] (and Table 2). Experimental data for the α / γ equilibrium quoted in [33] from unpublished sources [34–36] are reproduced in Table 4. Agreement with the authors' recommended isotherms at 1300, 1200 and 1000 °C (Fig. 4) is quite good.

Table 5 Atomic Sizes of Elements

Element	Crystal structure	Lattice spacing at 20 °C, nm	Closest interatomic distance, nm
Fe	bcc	0.28664	0.24823
Cr	bcc	0.28846	0.2498
Ni	fcc	0.35238	0.24919

Table 6 Lattice Spacings of $Cr_{1-x}Fe_xNi_3$ Alloys [37]

Composition Cr, at.%	Lattice spacing, nm	Density, gcm^{-3}
0	0.35561	8.61
5.5	0.35561	8.52
10.0	0.35543	8.51
14.1	0.35538	8.50
20.0	0.35547	8.47
24.1	0.35587	8.43

Lattice Spacings and Crystallography

All three elements have very similar atomic size, according to [Pearson] (see Table 5).

The solid phases in the ternary system, α, α', γ and σ, are all derived from the respective binary alloys: no ternary compounds have been found. Only the γ-phase has been systematically studied for the influence of heat treatment and composition on the lattice spacing which varies between 0.357 and 0.358 nm [10, 11].

The effect on ordering by substituting Cr for Fe in the $FeNi_3$ superlattice has been correlated with Young's modulus, density, electrical resistivity, and saturation magnetization [37–40]. Neutron diffraction showed that chromium, in common with many other metallic elements, reduces the long-range order parameter [40].

A redistribution of atoms during low-temperature aging was interpreted in terms of a change from long- to short-range ordering [37]. Lattice spacings and densities for $Cr_xFe_{1-x}Ni_3$, read from a small graph in [37], are given in Table 6. Lattice spacings for evaporated samples of α, σ and γ in ternary alloys may be found in [41] and [42]. The σ-phase is reported by [41] to extend over a very wide composition range in the ternary system that includes the Ni-Cr edge (confirming a theoretical prediction by [43] for the latter binary system), but the experimental conditions for its formation suggest it to be metastable, at least at temperatures of practical interest, and its bearing on the phase equilibria of the ternary system will not be considered further.

Acknowledgments

The Science Research Council must be thanked for a financial grant without which this project would not have been possible. The authors would also like to thank J. Vaughan and L. Jones of The Metals Society for generous assistance with a computer search of the literature, and A. Prince of the Hirst Research Centre, Wembley, and Dr. T. G. Chart, National Physical Laboratory, for their careful reviews of this paper.

Cited References

1. T. F. Connolly and E. D. Copenhaver, Bibliography of Magnetic Materials and Tabulation of Magnetic Transition Temperatures, IFI/Plenum, New York (1972).
2. A. H. Sully and E. A. Brandes, *Chromium*, 2 ed., p 77–82, Butterworths, London (1967).
3. E. C. Bain and W. E. Griffiths, *Trans. AIME*, *75*, p 166–213 (1927).
4. E. Schürmann and J. Brauckmann, *Arch. Eisenhüttenwes.*, *48*(1), p 3–7 (1977).
5. F. Wever and W. Jellinghaus, *Mitt. Kaiser-Wilhelm-Inst. Eisenforsch.*, *13*, p 98–109 (1931).
6. C. H. M. Jenkins, H. J. Tapsell, C. R. Austin and W. P. Rees, *J. Iron Steel Inst.*, *121*, p 266, 281 (1930).
7. C. H. M. Jenkins, E. H. Bucknall, C. R. Austin and G. A. Mellor, *J. Iron Steel Inst.*, *136*, p 187–222 (1937).
8. P. Schafmeister and R. Ergang, *Arch. Eisenhüttenwes.*, *12*(9), p 459–464 (1939).
9. A. J. Bradley and H. J. Goldschmidt, *J. Iron Steel Inst.*, *144*, p 273–288 (1941).
10. W. P. Rees, B. D. Burns and A. J. Cook, *J. Iron Steel Inst.*, *162*, p 325–336 (1949).
11. A. J. Cook and B. R. Brown, *J. Iron Steel Inst.*, *171*, p 345–353 (1952).
12. M. E. Nicholson, C. H. Samans and F. J. Shortsleeve, *Trans. ASM*, *44*, p 601–620 (1952).
13. A. M. Talbot and D. E. Furman, *Trans. ASM*, *45*, p (1953).
14. R. E. Lismer, L. Pryce and K. W. Andrews, *J. Iron Steel Inst.*, *171*, p 49–58 (1952).
15. L. Pryce, H. Hughes and K. W. Andrews, *J. Iron Steel Inst.*, *184*(3), p 289–301 (1956).
16. P. E. Price and N. J. Grant, *Trans. AIME*, *215*, p 635–637 (1959).
17. J. D. Jones and W. Hume-Rothery, *J. Iron Steel Inst.*, *204*, p 1–7 (1966).
18. B. Hattersley and W. Hume-Rothery, *J. Iron Steel Inst.*, *204*, p 683–701 (1966).
19. J. W. Schultz and H. F. Merrick, *Metall. Trans.*, *3*, p 2479–2483 (1972).
20. M. Hasebe and T. Nishizawa, Applications of Phase Diagrams in Metallurgy and Ceramics, Vol. 2, G. C. Carter, Editor, NBS special publication 496, p 910–954 (1978).
21. J. W. Pugh and J. D. Nisbet, *Trans. AIME*, *188*, p 268–276 (1950).
22. G. M. Gordon, Stress Corrosion Cracking and Hydrogen Embrittlement of Iron Base Alloys, Eds. R. W. Staehle *et al.*, National Association of Corrosion Engineers, Houston, Texas, p 893–945 (1978).
23. S. J. Rothman, L. J. Nowicki, and G. E. Murch, *J. Phys. F (Met. Phys.)*, *10*, p 383–398 (1980).
24. F. N. Rhines, *Phase Diagrams in Metallurgy*, McGraw-Hill, New York, p 151–153 (1956).
25. O. Kubaschewski and L. E. H. Stuart, *J. Chem. Eng. Data*, *12*(3), p 418–420 (1967).
26. S. W. Gilby and G. R. St. Pierre, *Trans. AIME*, *245*, p 1749–1758 (1969).
27. A. P. Lyubimov, A. A. Granovskaya and L. E. Berenshtein, *Nauch. Doklady Vyssh, Shkoly, Met.*, No. 1, p 7–10 (1958).
28. J. F. Counsell, E. B. Lees and P. J. Spencer, *Metallurgical Chemistry*, HMSO, London (1972).
29. L. Kaufman and H. Nesor, *Z. Metallkunde*, *64*(4), p 249–257 (1973).
30. L. Kaufman and H. Nesor, *Met. Trans.*, *5*(7), p 1617–1621 (1974).
31. F. Králík and K. Kováčóva, *Kovove Mater.*, *10*, p 380–381 (1972); *11*, p 6–15 (1973).
32. J. Vřeštal, A. Pokorna and A. Rek, *Kovove Mater.*, *14*, p 481–489 (1976).
33. M. Hillert and M. Waldenström, *Scand. J. Metall.*, *6*, p 211–218 (1977).
34. T. Ericsson, thesis, Royal Institute of Technology, Sweden (1962) (using commercial alloys).
35. A. Falkenö and H. Fredriksson, personal communication to [33].
36. B. Uhrenius and J. Hertsius, personal communication to [33].
37. L. P. Artsishevskaya, E. A. Ibragimov, Ya. P. Selisski and M. N. Sorokin, *Izv. Akad. Nauk SSSR Met.*, No. 4, p 158–164 (1968).
38. I. L. Eganyan and Ya. P. Selisski, *Akad. Nauk Ukr. SSR Metallofiz.*, No. 20, p 100–104 (1968).
39. I. L. Eganyan and Ya. P. Selisski, *Fiz. Met. Metalloved.*, *27*, p 210–218 (1969).
40. V. I. Gormankov, I. M. Puzei and E. I. Malt'sev, *Dokl. Akad. Nauk SSSR*, *194*, p 309–311 (1970).

Fig. 9 Calculated Isothermal Section for the Cr-Fe-Ni System at 900 K

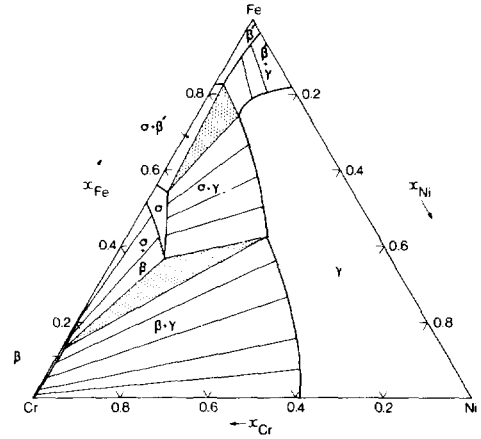

From [45].

41. N. Yukawa, M. Hida, T. Imura, M. Kawamura and Y. Mizuno, *Met. Trans.*, *3*, p 887–895 (1972).
42. N. Yukawa, M. Hida, T. Imura and Y. Mizuno, *Nippon Kinzoku Gakkai-Shi*, *35*, p 1100 (1971).
43. A. H. Sully, *Nature*, *167*, p 365–367 (1951).

Cr-Fe-Ni evaluation contributed by **G. V. Raynor** and **V. G. Rivlin**, Department of Physical Metallurgy and Science of Materials, University of Birmingham; extracted from [Rivlin/Raynor], bibliography through 1979.

Additional References

44. S. K. Mukherjee and D. Rogalla, The Effect of the Condensation Temperature on the Formation of Metastable Phases in Vapour-Deposited Fe-Ni-Cr Films and their Magnetic Properties, *Thin Solid Films*, *56*(3), p 279–290 (1979). (The effect of the Si substrate temperature on the width of the (α + γ) vapor-deposited 500 nm thick Cr-Fe-Ni films was studied from 77 to 673 K. Over the entire temperature range, the width of the (α + γ) region was found to be considerably less than in the equilibrium state)
45. T. Chart, F. Putland and A. Dinsdale, Calculated Phase Equilibria for the Cr-Fe-Ni-Si System – I Ternary Equilibria, *Calphad*, *4*(1), p 27–46 (1980). (Isothermal sections were calculated at 900, 800, and 700 K, using the NPL system, "ALLOYDATA". The 900 K section is shown in Fig. 9)
46. P. L. Lin, A. D. Pelton, C. W. Bale and W. T. Thompson, An Interactive Computer Program for Calculating Ternary Phase Diagrams, *Calphad*, *4*(1), p 47–60 (1980). (Calculated the 1800 K isothermal section for Cr-Fe-Ni, in agreement with [30], as an illustration of a new computational strategy known as the "base phase method")

The Cr-Fe (Chromium-Iron) System

51.996 amu 55.847 amu

Chromium and bcc iron dissolve in all proportions from Cr to Fe. The α and δ allotropes of Fe unite at over 12 wt.% Cr to form a continuous bcc solid solution, αδFe, stable at all temperatures up to the solidus. Consequently, the range of the fcc γ-phase is restricted. The element Cr is a stabilizer for αδFe but not γFe.

The phase diagram in Fig. 1 shows a simple liquidus and solidus which passes through a minimum at 1510 °C and about 18 wt.% Cr. Systematic measurements [1, 2] of the liquidus and solidus, up to about 30 wt.% Cr, are in excellent agreement. The data from [1] have been used in Fig. 1. Liquidus data at higher chromium contents are from [3]. [3] also gave liquidus and solidus data at all compositions from iron to chromium. However, the freezing range reported by [3] is wider than that found in either [1] or [2] – a fact attributed to insufficient annealing before heating-curve thermal analysis [4] – and his data for the chromium-rich solidus are not included in Fig. 1.

The equilibria at low temperatures (below 800 °C) are governed by the σ-phase [Hansen], [Elliott] and [Shunk]. The σ-phase is known to form congruently from α at 820 °C and 48 wt.% Cr, according to [Elliott]. At lower temperatures a eutectoidal decomposition to α and α′ takes place. The sluggishness of all reactions involving the σ-phase has made its bounding temperatures and compositions a matter of some dispute. From a review of existing experimental information, combined with thermodynamic calculation of Gibbs free energy differences at low temperatures, [4] submit that the true eutectoid temperature is as low as 440 ± 20 °C. In Fig. 1 the diagram of these authors is used in defining the low-temperature equilibria. It is conceded, however, that owing to the very small differences in Gibbs free energy between the competing phases, metastable α and α′ can easily form at the expense of σ at over 440 °C.

The data for the γ-loop (Fig. 2) are taken from [5]. The fall in the γFe → αFe transformation temperature as Cr is added to Fe is well established by [Hansen], and the

Fig. 1 Cr-Fe Phase Diagram

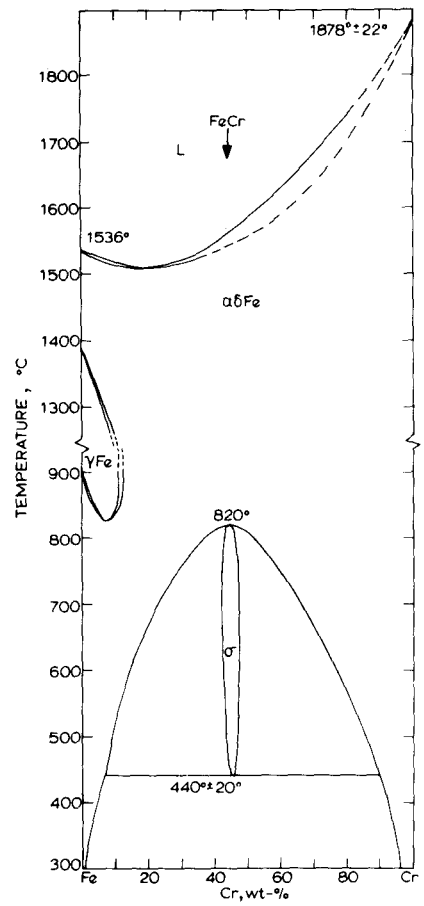

From [Rivlin/Raynor], 1980.